

Chlorophyll pigment concentration using spectral curvature algorithms: an evaluation of present and proposed satellite ocean color sensor bands

Frank E. Hoge and Robert N. Swift

During the past several years the symmetric three-band (460-, 490-, 520-nm) spectral curvature algorithm (SCA) has demonstrated rather accurate determination of chlorophyll pigment concentration using low-altitude airborne ocean color data. It is shown herein that the in-water asymmetric SCA, when applied to certain recently proposed OCI (NOAA-K and SPOT-3) and OCM (ERS-1) satellite ocean color bands, can adequately recover chlorophyll-like pigments. These airborne findings suggest that the proposed new ocean color sensor bands are in general satisfactorily, but not necessarily optimally, positioned to allow space evaluation of the SCA using high-precision atmospherically corrected satellite radiances. The pigment concentration recovery is not as good when existing Coastal Zone Color Scanner bands are used in the SCA. The in-water asymmetric SCA chlorophyll pigment recovery evaluations were performed using (a) airborne laser-induced chlorophyll fluorescence and (b) concurrent passive upwelled radiances. Data from a separate ocean color sensor aboard the aircraft were further used to validate the findings.

I. Introduction

The spectral curvature algorithm (SCA) is a three-band ratio type developed by Grew^{1,2} to calculate chlorophyll pigment concentrations from oceanic upwelled spectral radiances as measured by the Multichannel Ocean Color Sensor (MOCS). The computational technique was originally called the inflection ratio algorithm and was evaluated empirically over a 6-yr period using low-altitude MOCS data. The SCA results have been compared to (a) *in situ* data collected from surface vessels and (b) laser-induced chlorophyll fluorescence obtained with the NASA Airborne Oceanographic Lidar (AOL).¹⁻³ The high correlation between the SCA-derived and laser-fluorescence results (in addition to their agreement with ship-derived pigments) has produced a high degree of confidence in the three-band or spectral curvature method. Furthermore, a detailed study of the properties of the SCA³ has explained the physical basis for its success.

The SCA has shown such promise that some have inquired whether it could be (a) generally applied to the large amounts of existing CZCS data and/or (b)

used with the recently proposed satellite color bands on sensors that are due to replace or augment the aging CZCS. In this vein, still others have suggested that relatively minor changes in the placement of the usual two-band or blue-green algorithm bands, the SCA could be accommodated on future sensors without compromising or risking loss of the usual blue-green ratio data.

The purpose of this paper is to present the results of a study to assess the applicability of the SCA to (a) existing coastal zone color scanner (CZCS) bands and (b) new satellite sensors whose bands have been primarily selected for use with standard two-band or blue-green ratio algorithms. In turn it is then a secondary purpose of this paper to assess the optimality of the standard three-band symmetric SCA when compared to these asymmetrically occurring satellite band selections. The usual SCA for chlorophyll has center wavelength bands at 460, 490, and 520 nm. Hopefully, future experimental and theoretical studies will more fully address asymmetric chlorophyll SCAs.

Herein, when referring to passive measurements, chlorophyll, or chlorophyll pigments, is a generic term used to denote the sum of the concentration of chlorophyll *a* and the phaeopigments.

II. Spectral Curvature Algorithm

Grew¹ found that simple ratios of the sensor-measured radiances $L(\lambda)$ such as $L(\lambda_2)/L(\lambda_1)$ and $L(\lambda_3)/L(\lambda_2)$ tended to vary with environmental factors (such as

Frank Hoge is with NASA Goddard Space Flight Center, Wallops Flight Facility, Wallops Island, Virginia 23337; R. N. Swift is with EG&G Washington Analytical Services, Inc., Pocomoke City, Maryland 21851.

Received 24 March 1986.

Table I. Suitable Spectral Curvature Algorithm Center Bands for Chlorophyll C and Phycoerythrin P

Band	CZCS (Nimbus 7) Wavelength (bandwidth)	OCM (ERS-1) Wavelength (bandwidth)	OCI (NOAA-K) Wavelength (bandwidth)	OCI (SPOT-3) Wavelength (bandwidth)
1	443 (20)	400 (20)	443 (20)	443 (20)
2	520 (20)	445 (20)	490 (20) C	500 (20) C
3	550 (20)	520 (20) C	520 (20) C	565 (20)
4	670 (20)	565 (20)	565 (20)	665 (20)
5	750 (100)	640 (20)	620 (20) P	765 (40) ^a
6	11.5 μm (2 μm)	685 (20)	665 (20)	867 (45)
7		785 (30)	765 (40) ^a	
8		1020 (60)	867 (45)	
9		1600 (100)		11 μm (1 μm)
10		3700 (400)		12 μm (1 μm)
11		8500 (500)		
12		10800 (1000)		
13		12000 (1000)		

^a Notched for the 759–770-nm O₂ band.

solar elevation, sea state, and cloud cover). Here λ is the wavelength in the middle of a sensor band and $\lambda_1 < \lambda_2 < \lambda_3$ etc. However, a ratio of such ratios $L(\lambda_1)/L(\lambda_2) \div L(\lambda_3)/L(\lambda_1)$ varied significantly less. Thus he was led to investigate algorithms of the form

$$G_{mn}(\lambda_i) = \frac{L(\lambda_i)^2}{L(\lambda_{i-m}) \cdot L(\lambda_{i+n})}, \quad (1)$$

where $i = 1, 2, 3 \dots k$ represent the center channel or band number and m, n , the adjacent band number. For the MOCS, whose channels are separated by ~ 15 nm, Grew^{1,2} found that the most reliable indicator of chlorophyll concentration resulted from $i = 7$ and $m = n = 2$ or

$$G_{22}(\lambda_7) = \frac{L(490)^2}{L(460) \cdot L(520)}. \quad (2)$$

The actual form of the algorithm derived by Grew from comparisons with ship truth and airborne laser fluorescence is²

$$\log_e C = A - BG_{22}(\lambda_7), \quad (3)$$

where C is the chlorophyll a concentration in $\mu\text{g}/\text{liter}$. For an altitude of 150 m Grew found that the constants, $A = 10.19$ and $B = 7.33$, yielded the best results. However, the MOCS was uncalibrated at the time he established these coefficients. He found a correlation coefficient of $r = 0.985$ in a comparison with laser-induced fluorescence measurements² which were gathered simultaneously. For high altitudes, he used the same algorithm form but with considerably different values for the constant coefficients A and B . Although employed very successfully by Grew^{1,2} this algorithm is rather unconventional, since its form is exponential: $C = \exp[A - BG_{22}(\lambda_7)]$. Clearly, the chlorophyll concentration C is strongly driven by the numerical constants A and B as well as the $G_{22}(\lambda_7)$.

Campbell and Esaias³ used a more conventional ocean color algorithmic form for their study: $C = a_1 G^{b_1}$. [This form is more comparable to the $C = a_2 R^{b_2}$ type that is widely used in the usual two-band

(blue-green) ratio R methodology.^{4,5}] Campbell and Esaias³ analyzed the same data as Grew and obtained

$$\log_{10} C = a - b \log_{10} G_{22}(\lambda_7), \quad (4)$$

where $a = \log a_1 = 1.43$ and $-b = b_1 = 10.02$. On linear regression in the log-log domain a correlation coefficient $r = 0.94$ was found when applied to the same data for which Grew obtained the $r = 0.985$.

Campbell and Esaias³ found that their form of the algorithm is a measure of the curvature of the $\log_{10} S(\lambda)$ with respect to λ . It was further found that the algorithm effectively eliminates variations due to changes in incident irradiance while at the same time enhancing spectral features of the water medium. The irradiance reflectance of pure water exhibits a distinctive curvature spectrum with a large negative curvature³ at 490 nm. As chlorophyll-like pigments are added to the water this negative curvature monotonically approaches zero. This latter feature is the fundamental physical basis for the high sensitivity of the algorithm to chlorophyll in water.

The curvature algorithm is essentially a difference operator applied twice to the logarithm of the radiance in band i . At least two additional consequences result: (1) Since the differences (or amount of curvature) are small relative to the radiance at the three respective wavelengths, the sensor must possess rather high precision as well as a large dynamic range measurement capability. (2) The algorithm may be applied in real time (to uncalibrated data) obtained at low altitudes to obtain satisfactory chlorophyll measurements. The instrument must be stable enough to allow application of the constants determined previously. (Of course, at high-altitude, additive, independently varying, atmospheric path radiance must, as always, be first removed before the algorithm is applied to the three-band radiances. The work described herein uses airborne ocean color data obtained from 150-m altitude. Consequently, according to the results of Grew^{1,2} and the calculations of Campbell and Esaias³ atmospheric and sky reflectance corrections are not required and have not been applied.

Herein the general form of the algorithm as given in Eq. (4) will be used for all the analyses. The ability of this passive algorithm to recover chlorophyll-like pigments is assumed to be validated by the high correlation with laser-induced chlorophyll fluorescence obtained concurrently during the flight. Previous comparisons between the laser-induced and water-Raman-normalized chlorophyll fluorescence, and the surface truth chlorophyll measurements obtained from cooperating research vessels have established both the validity and linearity of the airborne fluorescence measurement.^{3,6}

III. Evaluation of Satellite Ocean Color Sensor Bands

Ocean color sensor data acquired from a low altitude (150 m) were used to evaluate the potential of existing and proposed ocean color bands for use in the curvature algorithm for chlorophyll measurement. Table I lists the satellite sensors and their spectral bands and

bandwidths (full width at half-maximum) considered in this study. The ocean color monitor (OCM) bands were obtained from a recent report.⁷ Having been launched in late 1978, the CZCS is presently still in operation. The ocean color imager (OCI) and the ocean color monitor (OCM) bands have received consideration for future launch. In our initial investigations we chose, for each of the above sensors, three spectral bands lying nearest to the usual 460-, 490-, and 520-nm wavelengths that have been generally applied to chlorophyll measurement with the curvature algorithm. Then all sequential three-band combinations were analyzed. The passive upwelled color spectra were interpolated to obtain the spectral radiance at the center of each of three satellite bands as given in Table I. The three radiance values were used to calculate

$$G = \frac{L(\lambda_2)^2}{L(\lambda_1) \cdot L(\lambda_3)},$$

where λ_2 is the central band center wavelength, and λ_1 and λ_3 are the center wavelengths of the adjacent shorter and longer wavelength bands, respectively. Over the entire flight line all the $\log G$ values were then regressed against the chlorophyll concentration. The relative chlorophyll concentration was determined from the laser-induced and water-Raman-normalized fluorescence simultaneously obtained with the passive ocean color spectra.

A. Instrumentation

The sensor used for this investigation was the NASA Airborne Oceanographic Lidar together with its integral passive ocean color subsystem (POCS). The AOL/POCS is an active-passive ocean color sensor since it provides both active and passive detection and quantification capabilities within a single instrument.^{8,9}

The active or lidar portion of the instrumentation has been discussed in detail in papers dealing with a number of diverse marine applications including chlorophyll mapping field experiments¹⁰⁻¹² as well as oil spill measurements,^{13,14} tracer dye concentration determination,¹⁵ oceanic turbidity cell structure,¹⁶ water depth,¹⁷ and laser backscatter^{18,19} measurement investigations. The AOL is also capable of performing terrestrial investigations^{20,21} including leaf fluorescence.²² For the experiments described herein, the instrument was configured as described in Refs. 8 and 9.

The airborne ocean color data were acquired from a NASA P-3A aircraft flying ~150 m above the ocean surface. The AOL final mirror was adjusted so that the ocean was viewed at an off-nadir angle of 15°. This off-nadir adjustment not only helped eliminate strong on-wavelength laser backscatter into the spectrofluorometer, but it was also used as an effective means in this study to reduce or eliminate specular reflection into the spectrometer. This was accomplished by azimuthally pointing the mirror so that the

system viewed the ocean 180° from the direction of the sun.

The AOL/POCS was calibrated using an integrating sphere similar to the one described by Hovis and Knoll.²³ This calibration is estimated to be accurate to $\pm 5\%$ level and removes the major radiometric differences among the various channels caused by individual photomultiplier tube (PMT) gain differences inherently established at the time of manufacture. Once the PMT voltages necessary for passive mode calibration were determined using the calibration sphere, the active mode was tested in a specific wavelength interval by radiating a fluorescent target with the 532-nm pulsed laser. Since only standard wide bandwidth electronic amplifiers and analog-to-digital (ADC) equipment immediately follow the PMTs, the active or lidar portion of the systems is estimated to be calibrated to the $\pm 10\%$ level. These aspects are discussed in considerably more detail in Ref. 8. This degree of active system calibration is quite adequate for the specific application utilized in this paper, since only a relative chlorophyll concentration is required. Adequate calibration and stability of the passive portion of the spectrometer are more important in this application, since any errors in the relative sensitivity between passive channels are leveraged by the power-law form of the curvature algorithm and thus are essentially the limiting factor in the analysis presented in this paper.

B. Experiment Description

The data given herein were acquired in the New York Bight during the conduct of airborne field experiments as part of the Department of Energy (DOE) sponsored shelf edge exchange processes (SEEP) investigations. The SEEP investigation conducted initially in the New York Bight region is designed to assess the assimilative capacity of the Continental Shelf along the East Coast to absorb energy by-products introduced into the near-shore ocean environment from coastal communities and marine activities, such as energy production plants and offshore oil operations. This capacity depends to a great extent on rates of removal by sinks in the marine ecosystem. Accordingly, the distribution and abundance of marine phytoplankton over the Shelf and in the adjacent slope water masses are of fundamental importance in this process. The initial SEEP studies, conducted between Feb. and May 1984, are part of a longer range program for the mid-Atlantic region which is planned to continue every 2 yr over the next decade. Other institutions participating in these field studies are Brookhaven National Laboratory (BNL), Yale University, LaMont Doherty Geophysical Observatory, and Woods Hole Oceanographic Institution. Oceanographic observations within the SEEP test area were acquired from ship (RV Endeavor), moored buoy, satellite, and aircraft platforms. The chlorophyll *a*, temperature, optical attenuation, and other shipboard measurements related to the AOL observations have not yet been fully analyzed. Likewise, the results from satellite imagery analysis and sensors deployed on the

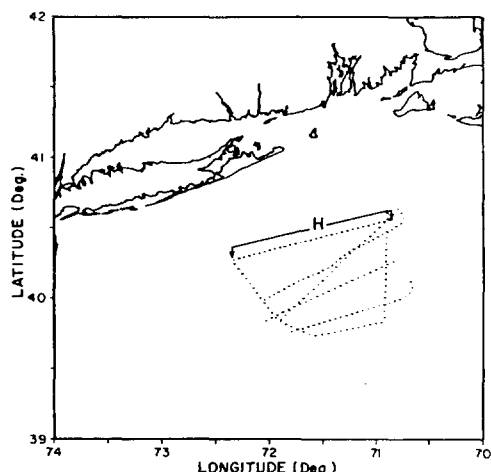


Fig. 1. Location of the SEEP field test site in the New York Bight where the airborne active and passive data were obtained. Line *H* had the highest pigment variability and was selected for the curvature algorithm study.

moored buoys have not yet been evaluated for comparison with the airborne data.

Data were chosen from the above regions to evaluate the satellite bands for chlorophyll recovery using the curvature algorithm.

V. Airborne Field Experiment Results and Analytical Approach

A flight line from the SEEP mission flown on 2 Apr. 1984 has been chosen to evaluate the potential of the CZCS and proposed OCI and OCM satellite bands. This mission is one of four flown during the SEEP studies. The 2 Apr. mission was flown 2 days after a moderate westerly wind flow was experienced in the area. A general increase in both the level and spatial variability of chlorophyll *a* concentration was observed following this event, especially in the inner portion of the SEEP study site.^{8,9} As will become immediately apparent in subsequent discussions, variability in chlorophyll concentration is an essential requirement for the technique used in this paper.

The flight lines flown during the 2 Apr. mission are shown in Fig. 1. The perimeter of the flight lines essentially defines the SEEP study site. The flight lines were designed in conjunction with BNL to complement their sampling strategy with the moored fluorometer arrays. The aircraft data provided periodic synoptic assessment of the chlorophyll *a* distribution between the buoys, especially along-shelf which was expected to be the dominant direction of surface current flow and, therefore, the net trajectory for entrained particulate matter.

The AOL/POCS was adjusted to yield thirty-two contiguous channels in the 408–768-nm spectral region. Each POCS spectrum was linearly interpolated to obtain the radiance corresponding to the center wavelength of the satellite bands listed in Table I. Satellite bands falling outside the nominal airborne POCS range (408–768 nm) were not considered. For example, no calculations were performed for the curva-

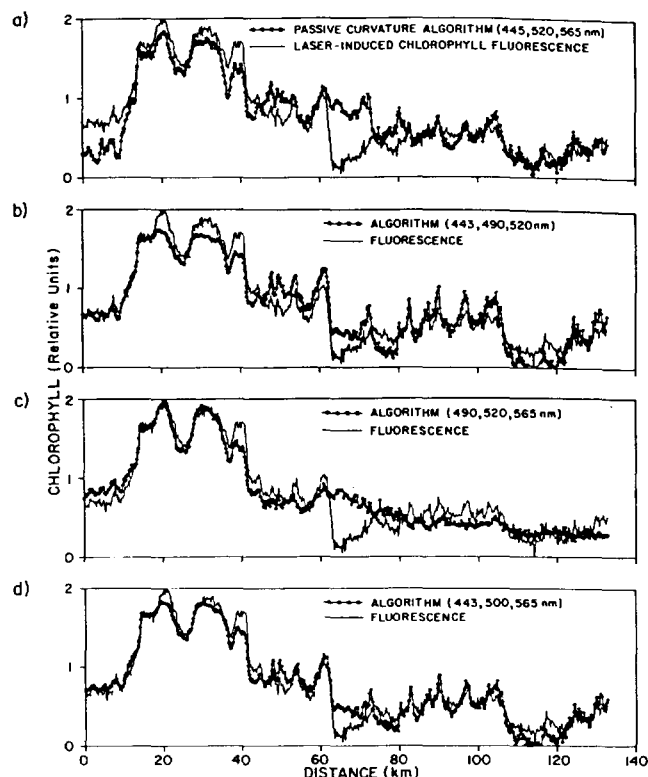


Fig. 2. Comparison of the spectral curvature algorithm with the laser-induced and water-Raman-normalized chlorophyll fluorescence: (a) OCM, ERS-1 (445, 520, 565 nm); (b) OCI, NOAA-K (443, 490, 520 nm); (c) OCI, NOAA-K (490, 520, 565 nm); (d) OCI, SPOT-3 (443, 500, 565 nm).

ture algorithm corresponding to the OCM 400, 415, 520 bands, since no airborne data were available for the 400-nm band. Also, no consideration was given to the bandwidth of the satellite band; i.e., the airborne POCS data were not integrated over the bandwidth of the satellite band, but instead only the radiance value at the center wavelength position was used. All possible curvature algorithms for nearest-neighbor satellite bands were used to calculate the chlorophyll concentration according to Eq. (4). Nonadjacent band algorithms were not considered. For example, an algorithm using the 443, 520, 670 bands of the CZCS was not investigated.

For each of the three-band combinations all 8000 of the log*G* values for the entire flight line *H* were linearly regressed against the laser-induced chlorophyll fluorescence. In Table I those algorithms having a correlation >0.9 are labeled *C* (for chlorophyll). In fact all four of these "acceptable" chlorophyll curvature algorithms had correlations of *r* = 0.94 or greater. These results suggest that any of these proposed satellite color band combinations could be used to study the effectiveness of the curvature algorithm as applied to spaceborne data. The four curvature algorithm results are each compared with the laser-induced fluorescence profile in Fig. 2. The results further suggest that the existing CZCS sensor bands are not as good. However, the 443-, 520-, 550-nm CZCS bands showed a

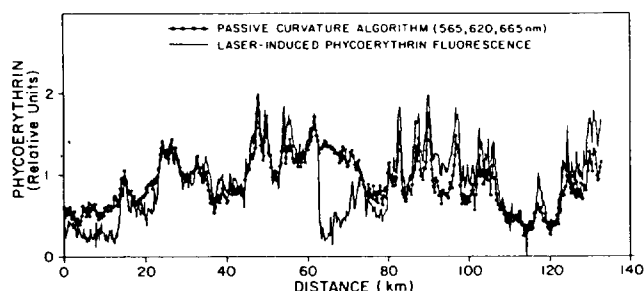


Fig. 3. Comparison of the 565-, 620-, 665-nm spectral curvature algorithm with the laser-induced and water-Raman-normalized phycoerythrin fluorescence.

$r = 0.87$ correlation, while the 550-, 670-, 750-nm bands yielded a 0.83 correlation. The highest chlorophyll *a* concentration was $\sim 3 \mu\text{g/l}$ at the 20-km position of the flight line. This concentration was determined by the standard chlorophyll algorithm in Eq. (3).

The AOL recorded the entire laser-induced spectrum which included the phycoerythrin fluorescence and water Raman backscatter. The same sequential band combinations previously used in the chlorophyll regression analysis were processed through the curvature algorithm and compared with both the phycoerythrin fluorescence and Raman backscatter. The 565, 620, 665 nm of the OCI (NOAA-K) curvature algorithm showed a correlation of $r = 0.85$ and is labeled P in Table I. This phycoerythrin algorithm is compared to the normalized laser-induced phycoerythrin fluorescence cross section in Fig. 3. No other available bands showed correlation $> r = 0.6$ for phycoerythrin. The water Raman backscatter showed no significant correlation with any possible curvature algorithm. Accordingly, no such labels appear in Table I.

Thus far, only the airborne active and passive data obtained in the New York Bight during the SEEP field experiments have undergone detailed study of satellite color band placement for photopigment estimation. As data from other oceanic regions becomes available, the general validity of the results obtained here can be more fully assessed.

IV. Summary and Conclusions

Over the past several years the spectral curvature algorithm has demonstrated very good chlorophyll (or chlorophyll-like) pigment concentration measurement results. The recovery of chlorophyll pigment by the spectral curvature algorithm has been tested using not only ship truth but also with simultaneous airborne laser-induced chlorophyll fluorescence measurements. The algorithm effectively eliminates variation due to changes in incident irradiance while at the same time enhances the spectral features of the water medium. Accordingly, the algorithm can be applied in real time to uncalibrated and uncorrected total sensor radiance data when such data are taken from low aircraft altitudes (~ 150 m). At higher altitudes additive atmospheric path radiance must first be removed before the algorithm is applied. For the advantages of such an

algorithm a price must be paid. The algorithm is essentially a difference operator applied twice to the logarithm of the upwelled radiances, and, since the result is a small difference in relatively large numbers, the sensor must possess reasonably high precision and channel-to-channel stability. Small errors (e.g., due to poor atmospheric correction) are "leveraged" into very large errors in chlorophyll estimates. Accordingly, it is recommended that the curvature algorithm be cautiously applied to the existing satellite sensor. For new satellite sensors, the necessary precision and stability are not unreasonable requirements and can be accomplished with the careful design engineering and fabrication attention normally given to a satellite sensor. Airborne instruments have already demonstrated the short-term stability and precision required with little attention focused on these aspects.

There is considerable inertia associated with existing and proposed sensor design. Difficulty is often encountered in effecting even small changes in the wavelengths for proposed satellite color sensors. Accordingly, the effectiveness of existing and presently designated bands was assessed when used with the curvature algorithm. The OCM (ERS-1), OCI (NOAA-K), and OCI (SPOT-3) band placements all are shown to provide at least one set of wavelengths that are spectrally located to provide spaceborne assessment of the chlorophyll spectral curvature algorithm. Furthermore, the OCI (NOAA-K) band selection yielded a promising phycoerythrin SCA when the 565-, 620-, and 665-nm bands are utilized.

It was found that the existing CZCS bands are not as satisfactorily positioned to yield chlorophyll pigment concentrations as are the proposed sensor bands of OCM and OCI. The 443-, 520-, 550-nm and 550-, 670-, and 750-nm CZCS bands yielded only a $r = 0.87$ and 0.83 correlation. The CZCS band SCAs also showed no significant correlation with phycoerythrin or water Raman backscatter.

A symmetric curvature algorithm centered at 600 nm recently yielded reasonably good recovery of the chlorophyll accessory pigment (CAP), phycoerythrin. It is hoped that new laser wavelengths will allow the stimulation of other accessory pigments and the subsequent development of passive ocean color algorithms to allow their airborne, and ultimately, satellite detection and mapping.

The authors wish to extend their personal thanks to the many persons involved with the scientific field experiments, the AOL project, and aircraft operations. We are particularly indebted to the Instrument Electro-Optics Branch for the loan of the frequency-doubled Nd:YAG laser used to obtain the active data. We also thank the Ocean Processes Branch of NASA Headquarters for continued support and encouragement. AOL system calibration assistance by the Sensor Evaluation Branch of GSFC and Warren Hovis and Jack Knoll of the NOAA National Environment Satellite Data and Information Service is gratefully acknowledged.

References

1. G. W. Grew, "Real-Time Test of MOCS Algorithm during Superflux 1980," in *The Chesapeake Bay Plume Study: Superflux 1980*, NASA CP 2188, J. W. Campbell and J. P. Thomas, Eds. (Langley Research Center, Hampton, VA, 1981).
2. G. W. Grew and L. S. Mayo, "Ocean Color Algorithm for Remote Sensing of Chlorophyll," NASA Tech. Paper 2164 (Langley Research Center, Hampton, VA, 1983).
3. J. W. Campbell and W. E. Esaias, "Basis for Spectral Curvature Algorithms in Remote Sensing of Chlorophyll," *Appl. Opt.* **22**, 1084 (1983).
4. H. R. Gordon and A. Y. Morel, "Remote Assessment of Ocean Color for Interpretation of Satellite Visible Imagery, A Review," in *Lecture Notes on Coastal and Estuarine Studies* (Springer-Verlag, New York, 1983), p. 30.
5. H. R. Gordon, D. K. Clark, J. W. Brown, R. H. Evans, and W. W. Broenkow, "Phytoplankton Pigment Concentrations in the Middle Atlantic Bight: Comparison of Ship Determinations and CZCS Estimates," *Appl. Opt.* **22**, 20 (1983).
6. F. E. Hoge and R. N. Swift, "Application of the NASA Airborne Oceanographic Lidar to the Mapping of Chlorophyll and Other Organic Pigments," in *Chesapeake Bay Plume Study Superflux 1980*, NASA Conf. Publ. 2188 (U.S. GPO, Washington, DC, 1981), p. 349.
7. "Ocean Color Working Group," a progress report to ESA Earth Observation Advisory Committee, European Space Agency Report ESA BR-20, Paris, France, June 1984.
8. F. E. Hoge, R. E. Berry, and R. N. Swift, "Active-Passive Airborne Ocean Color Measurement. 1: Instrumentation," *Appl. Opt.* **25**, 39 (1986).
9. F. E. Hoge, R. N. Swift, and J. K. Yungel, "Active-Passive Airborne Ocean Color Measurement. 2: Applications," *Appl. Opt.* **25**, 48 (1986).
10. F. E. Hoge and R. N. Swift, "Airborne Simultaneous Spectroscopic Detection of Laser-Induced Water Raman Backscatter and Fluorescence from Chlorophyll *a* and Other Naturally Occurring Pigments," *Appl. Opt.* **20**, 3197 (1981).
11. F. E. Hoge and R. N. Swift, "Application of the NASA Airborne Oceanographic Lidar to the Mapping of Chlorophyll and Other Organic Pigments," in *Chesapeake Bay Plume Study Superflux 1980*, NASA Conf. Publ. 2188 (U.S. GPO, Washington, DC, 1981), p. 349.
12. F. E. Hoge and R. N. Swift, "Airborne Dual Laser Excitation and Mapping of Phytoplankton Photopigments in a Gulf Stream Warm Core Ring," *Appl. Opt.* **22**, 2272 (1983).
13. F. E. Hoge and R. N. Swift, "Experimental Feasibility of the Airborne Measurement of Absolute Oil Fluorescence Spectral Conversion Efficiency," *Appl. Opt.* **22**, 37 (1983).
14. F. E. Hoge and R. N. Swift, "Oil Film Thickness Measurement Using Airborne Laser-Induced Water Raman Backscatter," *Appl. Opt.* **19**, 3269 (1980).
15. F. E. Hoge and R. N. Swift, "Absolute Tracer Dye Concentration Using Airborne Laser-Induced Water Raman Backscatter," *Appl. Opt.* **20**, 1191 (1981).
16. F. E. Hoge and R. N. Swift, "Airborne Detection of Oceanic Turbidity Cell Structure Using Depth-Resolved Laser-Induced Water Raman Backscatter," *Appl. Opt.* **22**, 3778 (1983).
17. F. E. Hoge, R. N. Swift, and E. B. Frederick, "Water Depth Measurement Using an Airborne Pulsed Neon Laser System," *Appl. Opt.* **19**, 871 (1980).
18. F. E. Hoge, W. B. Krabill, and R. N. Swift, "The Reflection of UV Laser Pulses from the Ocean," *Mar. Geod.* **8**, Nos. 1-4, 313 (1984).
19. J. L. Bufton, F. E. Hoge, and R. N. Swift, "Airborne Measurements of Laser Backscatter from the Ocean Surface," *Appl. Opt.* **22**, 2603 (1983).
20. W. B. Krabill, J. G. Collins, L. E. Link, R. N. Swift, and M. L. Butler, "Airborne Laser Topographic Mapping Results," *Photogram. Eng. Remote Sensing* **50**, 685 (1984).
21. R. Nelson, W. B. Krabill, and G. Maclean, "Determining Forest Canopy Characteristics Using Airborne Laser Data," *Remote Sensing Environ.* **15**, 201 (1984).
22. F. E. Hoge, R. N. Swift, and J. K. Yungel, "Feasibility of Airborne Detection of Laser-Induced Fluorescence Emissions from Green Terrestrial Plants," *Appl. Opt.* **22**, 2991 (1983).
23. W. A. Hovis and J. S. Knoll, "Characteristics of an Internally Illuminated Calibration Sphere," *Appl. Opt.* **22**, 4004 (1983).